

## UWB-Radar-Sensed Human Respiratory Signal Modeling Based on the Morphological Method

Miao Liu<sup>1, 2, †</sup>, Huijun Xue<sup>1, †</sup>, Fulai Liang<sup>1, †</sup>, Hao Lv<sup>1</sup>,  
Zhao Li<sup>1</sup>, Fugui Qi<sup>1</sup>, Ziqi Zhang<sup>1</sup>, and Jianqi Wang<sup>1, \*</sup>

**Abstract**—This paper proposes a morphological ultra-wideband (UWB)-radar-based respiratory signal model. According to the detection theory, it is crucial to set up an appropriate model to fulfil the detection purpose. Previous models pay less attention to the time dimension of the respiratory signal, but the frequency domain cannot precisely describe it because of its non-linearity and non-stationarity. This model uses a morphological operator to dilate or erode the base wavelet, and the length and value of the digit in the structure element serve as the parameters in this morphological model. The result of the experiment carried out on 10 human targets with impulse radio ultra-wideband (IR-UWB) radar proves the efficiency of this model. As the UWB radar sensed human respiratory signal is nonlinear and non-stationary, the parameters in the model can be regarded as a measure of non-linearity and non-stationarity. An experiment is carried out with the simulated respiratory signal generated with the proposed model. The result shows that the detection algorithm based on Ensemble Empirical Mode Decomposition (EEMD) method has a better performance than that based on Adaptive Line Enhancer (ALE) and with the value of the digit in the structure element increases, the performance of the ALE method declines, while the EEMD method stays in a good performance, which indicates that the EEMD method has a good potential to deal with the nonlinear and non-stationary respiratory signal.

### 1. INTRODUCTION

UWB radar has the advantages of non-contactness and penetrability through non-metallic materials. It can be used to detect the human beings in the scenarios of search and rescue, anti-terrorism and some other important areas [1–8]. The electromagnetic wave is radiated by the transmitting antenna and reflected back by the human body. The human target can be detected and located by analyzing the micro-motion hidden in radar echoes, which means that the aim of detecting human beings is usually achieved by detecting the respiration and heartbeat of human body. According to the detection theory, it is important to set up the to-be detected signal model to ensure the effectiveness of the detection [9]. Therefore, the accuracy of the model of the respiration and heartbeat affects the UWB radar human detection. As the amplitude of the movement caused by the respiration is about 10 times larger than that caused by the heartbeat, the paper focuses on the model of the respiratory signal.

As a quasi-periodic signal, the respiratory signal is usually modeled as a sinusoid signal with the parameters of amplitude, frequency and phase. But the shape of the respiratory signal is not always in a sinusoid, then a model based on the even power of cosine function (EPCM) and the power of absolute value of cosine function (PACM) is proposed [10]. However, like other biomedical signals, respiratory signal is a kind of nonlinear and non-stationary signal. The parameters of the signal change with time, so does the waveform of the signal. But as the respiratory signal is generated from the same person in a

---

Received 26 September 2018, Accepted 21 November 2018, Scheduled 4 December 2018

\* Corresponding author: Jianqi Wang (wangjq@fmmu.edu.cn).

<sup>1</sup> School of Biomedical Engineering, The Fourth Military Medical University, Xi'an 710032, China. <sup>2</sup> The General Hospital of Shenyang Military Region, PLA, Shenyang 110016, China. <sup>†</sup> These authors contributed equally to this work.

certain time period, the general waveform shapes in a certain time are identical. According to the theory of mathematical morphology, the morphological method like dilation and erosion can change the wave shape in an extent determined by the structure element [11]. The mathematical morphological method is widely used in different areas. In the two-dimensional data processing area, it is used in image processing and segmentation. As to one-dimensional data processing area, it is used in biomedical signal detection and extraction [12–14]. Because the waveform of the one dimensional respiratory signal changes among different periods, it is suitable to be modeled by morphological method with the parameters being the structure element. Therefore, a new respiratory signal model based on the morphological method is proposed, and the model is verified by the signal in the database. An experiment is carried out with an IR-UWB radar. To further testify the influence of the model parameters on the detection algorithms, a simulated experiment is carried out with two detection algorithms.

The rest of the paper is arranged as follows. Section 2 illustrates the mathematical model of the respiratory and the verification of the model. Section 3 depicts the varying parameters' effect on the detection algorithms. Finally, the discussion and conclusion are given in Section 4 and Section 5.

## 2. MORPHOLOGICAL MODEL OF RESPIRATORY SIGNAL

### 2.1. The PACM Model

There are mainly 4 respiratory signal modeling methods, which are listed in Table 1 [10]. The CM is a cosine model, which just models the respiratory signal with cosine function and treats it as a plain cosine signal. The ACM is an absolute cosine model, which uses the absolute value of the cosine function and is shown to be more accurate than the CM model [15]. The EPCM is an even power cosine model, which takes the duty cycle into account, and it depends on the parameter  $m$ . It has better performance than

**Table 1.** Various respiratory signal models.

Model	Respiratory Signal
CM Model	$M_c^{(f,d_c,A_c)}(t) = d_c + A_c \cos(2\pi ft)$
AC Model	$M_{AC}^{(f,d_{AC},A_{AC})}(t) = d_{AC} - A_{AC} \cos(\pi ft) $
EPC Model	$M_{EPC}^{(f,d_{EPC},A_{EPC},m)} = d_{EPC} + A_{EPC}(\cos(\pi ft))^{2m}$
PAC Model	$M_{PAC}^{(f,d_{PAC},A_{PAC},n)}(t) = d_{PAC} + A_{PAC} \cos(\pi ft) ^n$

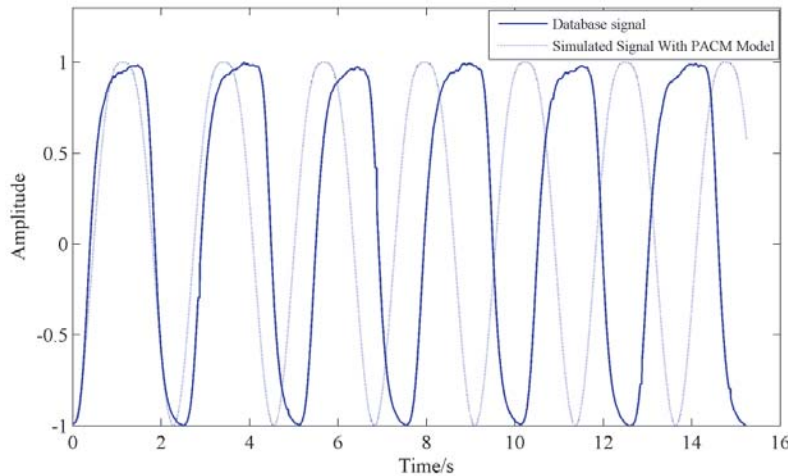


**Figure 1.** Database signal and simulated signal with PACM model.

the ACM model. The PACM is power of absolute value of cosine model, which avoids the disadvantage of the duty cycle deviation to some extent, showing a better performance than EPCM model.

With PACM model, the respiratory signal can be modeled by the respiratory frequency,  $f$ , power order,  $n$ , and the power of absolute value of cosine function.  $d_{PAC}$  is a DC term, which will be eliminated in the analysis of UWB echo signal.

The standard to evaluate the efficiency of a model is whether the model can mimic the respiratory signal with the optimized parameters. The data used for model performance test are the benchmark dataset from CapnoBase, which is a public database for respiratory signal analysis [16]. It is measured by capnography, highly correlated with respiratory volume, which can be measured by respiration belt [17]. The simulated respiratory signal frequency is set by the FFT analysis to the database signal, and the time duration is set by the equation that the data number of the database signal is divided by the sampling frequency. Both of the simulated signal and database signal are scaled into the amplitude range of  $[-1, 1]$ . The result is shown in Figure 1.

It can be seen from Figure 1 that the simulated respiratory signal cannot mimic the database signal well because of the non-linearity and non-stationarity of the respiratory signal.

## 2.2. Mathematical Morphology

Mathematical morphology has been mostly applied to image processing area, and one dimensional morphology operators have been used for line detection and path opening etc. It is a process directly carried out on the time or space domain.

The theory of mathematical morphology is based on mathematical operators, which are applied to the analyzed signal with structure elements. Structure element is a predefined shape, such as flat and triangle, with finite length. The mathematical morphology process is a new signal construction process through sliding the line segment ( $G$ ) along the original signal ( $F$ ) to trace out the new signal.

There are four basic mathematical morphology operations:

Dilation:

$$(F \oplus G)(x) = \bigvee_{h \in [a,b]} F(x-h) \quad (1)$$

Erosion:

$$(F \ominus G)(x) = \bigwedge_{h \in [a,b]} F(x+h) \quad (2)$$

Opening:

$$(F \circ G)(x) = ((F \ominus G) \oplus G)(x) \quad (3)$$

Closing:

$$(F \bullet G)(x) = ((F \oplus G) \ominus G)(x) \quad (4)$$

where  $[a, b]$  represents the integer range from  $a$  to  $b$  [11].

## 2.3. The Mathematical Model Based on Mathematical Morphology

Considering the similarity of the respiratory waveforms in different periods, the difference is mostly caused by the scale, which makes applying the theory of morphology to the mathematical modeling of respiratory signal possible. Because the respiratory signal is a time series, the one-dimensional morphological process reflects on the change of amplitude. With dilation processing, the signal can be amplified in some degree. In contrast, the signal can be lowered in amplitude with erosion processing. To some extent, the dilation and erosion processing are similar to amplification and shrinking respectively for a one-dimensional signal. However, the processing carried out on the signal should not only change the amplitude of the each signal datum individually, but also change the ratio relationship between the data, or the dilation and erosion will not take effect because of the scaling process.

First, consider the respiratory signal as a summation of different waveforms;  $f[n] = \sum_{k=1}^K \psi_k$ ,  $\psi_k$  represents the  $k$ th waveform;  $K$  is the total number of the waveforms. In order to easily decompose the respiratory signal into different waveforms, the waveforms are separated by the minimums. As to each

waveform, it is a transform of a base form, namely a base wavelet. With the dilation or erosion to the base wavelet, the new waveform is generated.

There are many ways to fulfill the morphology process, and the most common one is illustrated as follows,

$$g(n) = \max \{f(n + t) + s(t) | (n + t) \in D_f, t \in D_s\} \tag{5}$$

$$h(n) = \min \{f(n + t) - s(t) | (n + t) \in D_f, t \in D_s\} \tag{6}$$

$g(n)$  and  $h(n)$  denote the dilated and eroded signals respectively, and  $D_f$  and  $D_s$  denote the generated signal and structure element domain, respectively. It is clear that if the structure element, namely  $s(t)$ , has the form of  $[B B \dots B B]$ , whose elements are equal in value, and the value after process will always be  $f(n) + B$  when it is dilation and  $f(n) - B$  when it is erosion. Though the amplitude of the data can be amplified or reduced after the common morphological processing, the scaled results will not change with the value in the structure element.

Instead of the flat form of structure element, the structure element can also be in triangular form and some other forms, but changing the form of the structure element may result in the distortion of the shape of the signal, and it is hard to choose an appropriate form to model the respiratory signal. In order to keep the form of the structure element flat, as well as fulfill the goal of dilation and erosion, a novel morphological method should be proposed to satisfy this need, which can make the scaled signal change with the value in the structure element. Then not only the structure element should relate with the datum under processing, but also the datum or data nearby should be taken into account. The derivative of a time series measures the sensitivity to change of the signal value with respect to change of time, a novel morphological method based on derivative-based structure element is proposed,

$$g(n) = \max \{f(n) + [f(a) - f(a - 1)] * B | a \in [n - (A - 1)/2, n + (A - 1)/2]\} \tag{7}$$

Because the derivative varies within the window length determined by the length of structuring element, namely  $A$ , a changing  $B$  in the structure element can bring up different added or subtracted values according to the derivative, so as the scaled data changes with the value of  $A$  and  $B$  in the structure element. The results are shown in Figure 2 and Figure 3. Figure 2 is the result illustrating the effect of varying  $A$ , while Figure 3 is the result depicting the effect of varying  $B$ .

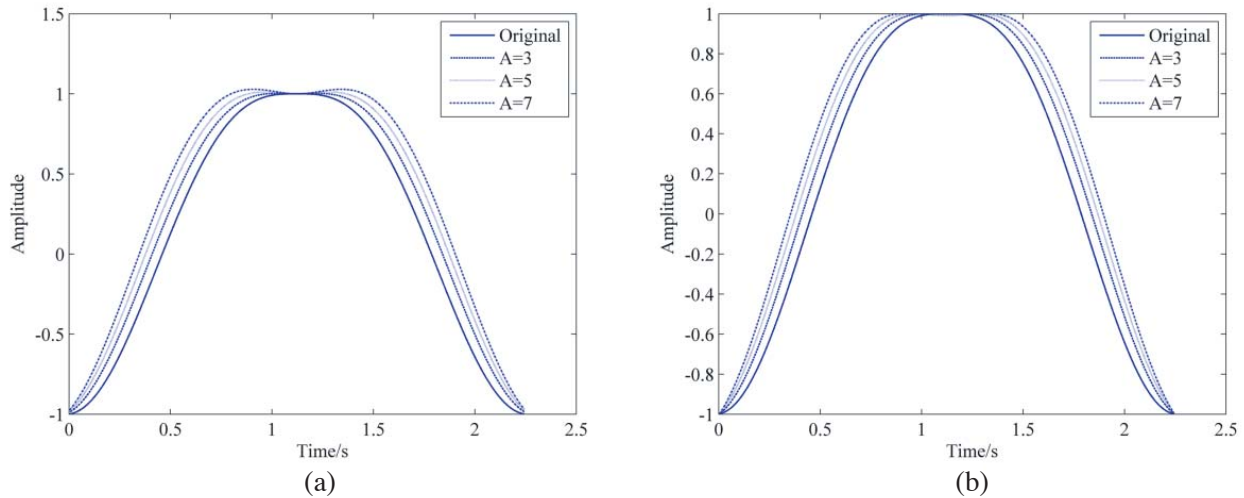


**Figure 2.** The effect of the length of structure element on the base wavelet. (a) The original base wavelet and signals after the novel dilation method; (b) The scaled original base wavelet and signals after the novel dilation method.

It can be seen that the shape of the scaled signal changes with the variant  $A$  and  $B$ . Though the shape can change with  $A$  and  $B$ ,  $A$  and  $B$  are both necessary for the model as  $A$  must be an integer and acts as a rough modeling parameter. When it is set,  $B$  acts as a delicate modeling parameter to further detail the respiratory signal.

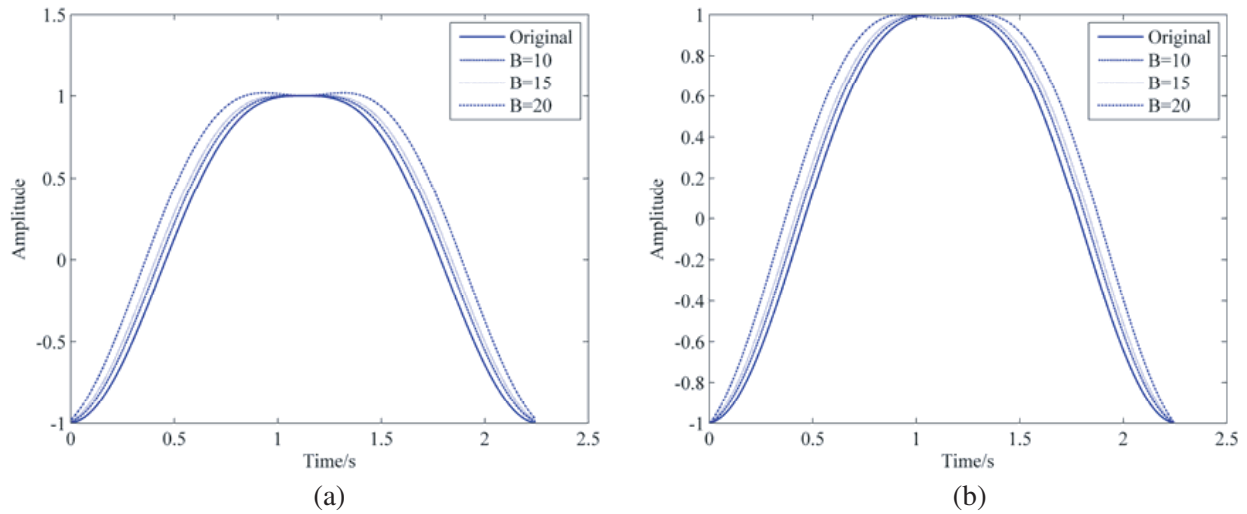


**Figure 3.** The effect of the value of structure element on the base wavelet. (a) The original base wavelet and signals after the novel dilation method; (b) The scaled original base wavelet and signals after the novel dilation method.

All in all, the modeling problems of nonlinearity and non-stationarity are solved by the minimum segmentation and mathematical morphological processing. Then the final form of the respiratory signal modeling is

$$g(n) = \sum_{k=1}^K \max \{ f(n) + [f(a) - f(a - 1)] * B | a \in [n - (A - 1)/2, n + (A - 1)/2] \}$$

$$\begin{cases} n = n_k & k = 1 \\ n = \sum_{k=1}^K k_N + n_k & k > 1 \end{cases} \tag{8}$$

in which  $n_k$  is the  $n$ th number in the  $k$ th waveform, and it will be a dilation process if  $B$  is positive and an erosion process if  $B$  is negative.

So the simulated respiratory signal is determined by  $K$ , which is the number of segmented waveforms,  $k_N$ , which is the number of data in the  $k$ th waveform,  $A$ , which is the length of the morphological process, and  $B$ , which is the value of the flat structuring element. Concerning the base waveform, it is set up by the PACM model described above.

### 2.4. Verification of the Morphological Model

The standard for evaluating the proposed model is the correlation coefficient between the real respiratory signal and the simulated respiratory signal with the optimized parameters listed above. The correlation coefficient, which is a measure of the correlation of two signals, is defined as the following equation

$$\rho_{XY} = \frac{\text{Cov}(X, Y)}{\sqrt{D(X)}\sqrt{D(Y)}} \tag{9}$$

where  $X, Y$  are two time series;  $\text{Cov}(X, Y)$  is the covariance of  $X$  and  $Y$ ;  $D(X)$  and  $D(Y)$  are squared deviations of  $X$  and  $Y$ , respectively.

#### 2.4.1. Experiment Setup

An experiment was carried out to collect the UWB radar sensed human respiratory signal at the Bioradar laboratory at the Fourth Military Medical University. 5 male and 5 female healthy volunteers

**Table 2.** Key parameters of IR-UWB radar.

Parameter	Value
Signal mode	Impulse
Transmission peak power	0.26 W
Pulse repetition frequency	128 kHz
Operating frequency	250–750 MHz
Receive dynamic range	80 dB
Receiver sensitivity	3 dB
ADC accuracy	16 bits
Minimum step	10 ps

are recruited in this experiment. Each volunteer is asked to stand behind a brick wall, whose thickness is 24 cm, breathing freely. An IR-UWB radar system consists of a transmitting antenna, and a receiving antenna, whose key parameters are listed in Table 2, is deployed on the wall at the other side. The IR-UWB radar system is with center frequency of 500 MHz and bandwidth of 500 MHz, which ensures good penetrability and high range resolution. It complies with the definition of UWB according to the federal communication commission (FCC). The pulse repetition frequency (PRF) is 128 kHz, and the transmit power is 0.26 W, which is safe to the experiment subjects. In addition, the radar is controlled by a laptop, and the data stream is transported through Wi-Fi. The distance between the human subject and the antenna was 3 m. The experiment scenario is depicted in Figure 4.

**Figure 4.** Experiment scenario of human respiratory signal detection based on IR-UWB radar, Tx is transmitting antenna, Rx is receiving antenna.

The IR-UWB radar echoes are received by the receiver antenna, sampled by the AD converter and then stored in the laptop in the form of data matrix. The radar echo signal is stored in a form of two-dimensional data  $r[m, n] = r[m\delta_\tau, nT_s]$ , where  $0 \leq m \leq M - 1$  and  $0 \leq n \leq N - 1$ . The column of the matrix represents a range profile of the IR-UWB radar data denoted as  $r_n[m]$ . The row of the matrix represents an echo signal at a range denoted as  $r_m[n]$ .  $\delta_\tau$  and  $T_s$  are the sampling interval in range (unit is nano second) and the measuring period in time (unit is second) [18].

#### 2.4.2. Model Parameter Estimation

In order to generate the waveform to best mimic the sensed respiratory signal, optimized parameters should be estimated. A flowchart of the model parameter estimation is depicted in Figure 5.

Firstly, detect and locate the human target by the Adaptive-multichannel singular spectrum analysis (MSSA) method and determine the range number  $m$  [19]. Extract the row signal  $r_m[n]$

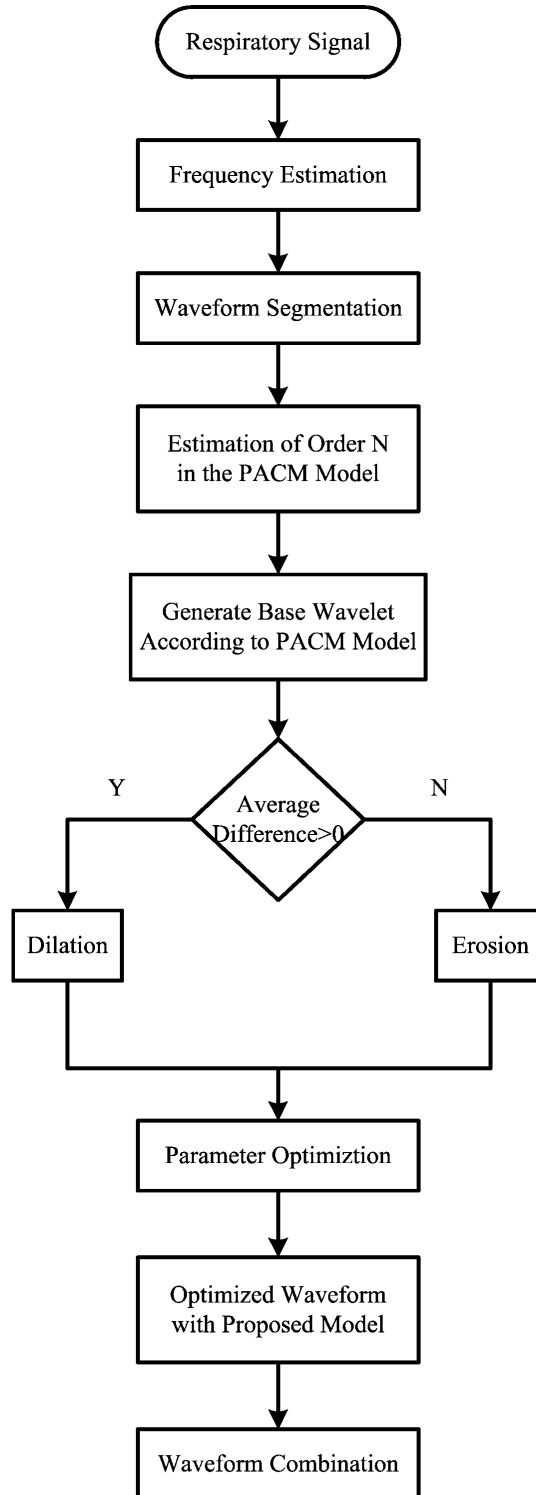


**Figure 5.** Flowchart of the morphological model parameter estimation.

and regard it as the respiratory signal data sensed by the IR-UWB radar. Afterwards, analyze it by FFT process, and the frequency is estimated. Then segment the signal into various waveforms by the minimums. Estimate the power order  $n$  which makes the correlation coefficients largest between the simulated and real respiratory signal. With the frequency and power order, a base wavelet can

be generated with the PACM model. Compare the segmented waveform with the base wavelet, if the average difference is larger than 0, then a dilation process should be used; otherwise, an erosion process should be used. As to the parameters of dilation or erosion, namely the length of structure element,  $A$ , and the value in it,  $B$ , a changing  $A$  (should be odd integer) from 3 to 21 and a changing  $B$  from 0.5 to 100 are applied to the morphological process. With each  $A$  and  $B$ , a correlation coefficient is calculated, and find  $A$  and  $B$  that make the correlation coefficient largest. The chosen  $A$  and  $B$  form an optimized structure element, and use this structure element to fulfill the morphological process. An optimized waveform is formed. The same process should be carried out on the other waveforms, and a sequence of optimized waveforms is generated. Sequence these waveforms up and fulfill the waveform combination process.

### 2.4.3. Experiment Results

Take one subject as an example to illustrate the calculating process and the result. The respiratory frequency is 0.5 Hz according to the FFT analysis. In the power order estimation procedure, the result is shown in Figure 6. It can be seen that the correlation coefficient changes with the order  $n$ , and when the  $n$  reaches 3, the correlation coefficient is at its largest value.

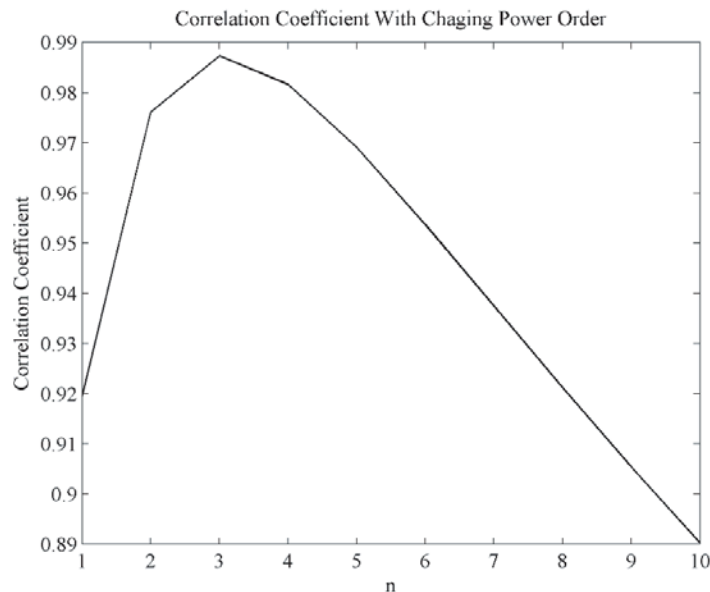


**Figure 6.** The result of power order estimation.

The respiratory signal was separated into 9 wavelets, and there will be 9 pairs of optimized parameters to form the structure element. The parameters are listed in Table 3.

With the respiratory frequency and the optimized power order, a base wavelet is formed with the PACM model. Compare the original PACM model and the proposed mathematical morphology model, and the results are shown in Figure 7 and Figure 8.

It can be seen that the proposed model can better mimic the respiratory signal, and the correlation coefficients can reach to 0.98, while that for the PACM model can only be 0.81.

It can be seen from Table 3 that the value of 2 takes most part of  $A$ , if we choose 2 as a fixed value for  $A$ , and the optimized  $B$  to best mimic the respiratory signal is  $-8, -12.5, -5.5, -6, -7, 3, -22.5, -9, -16.5$ .

Simulate a signal with fixed  $A$  and optimized  $B$ , the simulated signal is shown in Figure 9. The correlation coefficient between the real respiratory signal and simulated signal is 0.96. Though it is smaller than that with the optimized  $A$  and  $B$ , which is 0.98, it is larger than that with no optimized  $A$  and  $B$ , which is 0.81. It can be concluded that the simulated respiratory signal can better mimic the

**Table 3.** The result of parameter estimation.

Wavelet Number	$A$	$B$
1	2	-8
2	2	-12.5
3	1	-4.5
4	3	-7
5	9	-11.5
6	1	3.5
7	10	-28
8	1	-8
9	2	-16.5

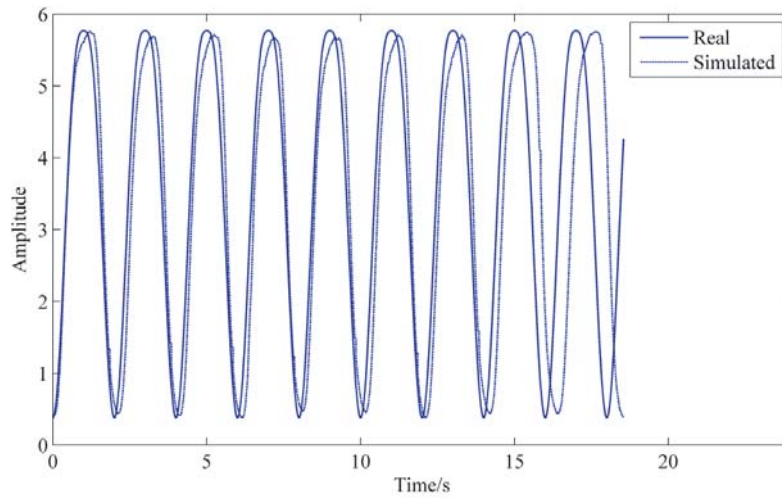


**Figure 7.** The comparison between the real respiratory signal and simulated signal with PACM model.

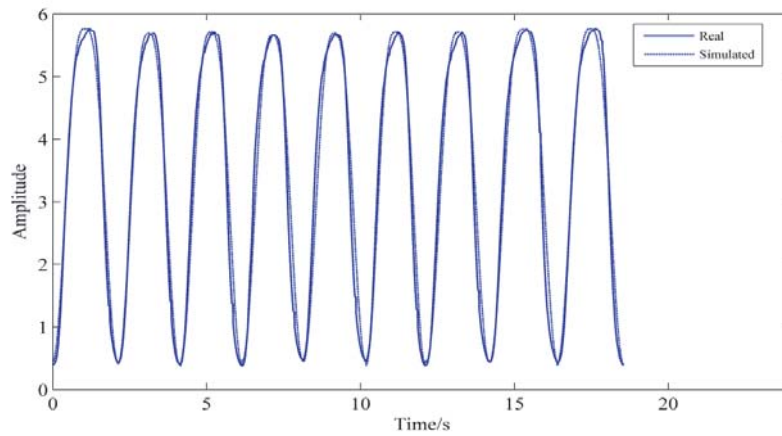


**Figure 8.** The comparison between the real respiratory signal and simulated signal with the proposed model.

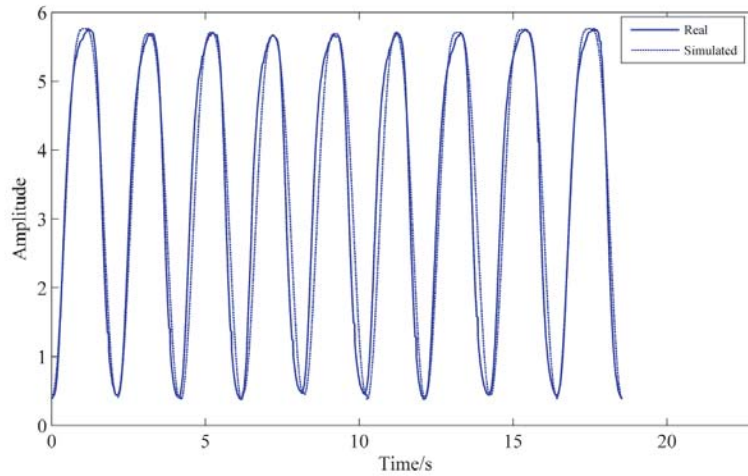


**Figure 9.** The comparison between the real respiratory signal and simulated signal with the proposed model with a fix length of structure element.

**Table 4.** The correlation coefficient with the two methods of the 10 subjects.

Subject	Correlation Coefficient	
	Proposed Method	PACM Method
Male 1	0.96	0.83
Male 2	0.97	0.78
Male 3	0.98	0.81
Male 4	0.94	0.82
Male 5	0.95	0.83
Female 1	0.89	0.81
Female 2	0.96	0.90
Female 3	0.86	0.76
Female 4	0.95	0.83
Female 5	0.97	0.82

real respiratory signal than the original PACM model, though the result is not as good as that with a varying  $A$ .

The experiment results of the 10 subjects are shown in Table 4, from which we can see that the proposed morphological method shows better performance than the PACM, because non-linearity and non-stationarity are taken into account. We can also see that some correlation coefficients are lower than 0.9, in spite of being applied with the proposed modeling method. This is caused by the random distortion of the waveform because of the micro-motion of the human target, which is hard to predict in advance.

### 3. MODEL'S EFFECT ON THE DETECTION ALGORITHMS

The proposed method models the UWB-radar sensed human respiratory signal with a sliding structure element applied to the base wavelet. The structure element is in a flat form with two parameters in it: one is the length, and the other is the value in it. In an extent, the two parameters can measure the non-linearity and non-stationarity of the UWB-radar sensed human respiratory signal. The non-linearity and non-stationarity are the main properties of the UWB radar sensed human respiratory

signal, compared with plain sinusoid signal.

Adaptive Line Enhancer (ALE) and Ensemble Empirical Mode Decomposition (EEMD) are two up-to-date human target detection methods based on the UWB radar. Now that the proposed modeling method can better mimic the UWB radar human respiratory signal, a set of respiratory signals are generated with it. And an experiment is carried out to test which algorithm has a better performance on extracting the respiratory signal with these simulated respiratory signals. A deviation of the parameters will be considered as a variable, and the detection effect with this variable is studied. We fix  $A$  in the structure element as 3 and change  $B$  to test the parameter's effect on the detection algorithm. A series of  $B$  is generated with a random function which can set the variance of this series. Combine the series of waveforms into a time series and add Gaussian noise into the combined time series.

The correlation coefficient is used as an index to test the performance of the algorithms. The larger the correlation coefficient is, the more performance the detection algorithm has.

### 3.1. Detection Algorithms Description

The first algorithm is adaptive line enhancer (ALE), which is a method for the detection of sinusoid signals in wideband noise [20]. It can adaptively cancel out the noise because the respiratory signal has strong self-correlated properties compared with the noise. A block diagram of the ALE is shown in Figure 10.

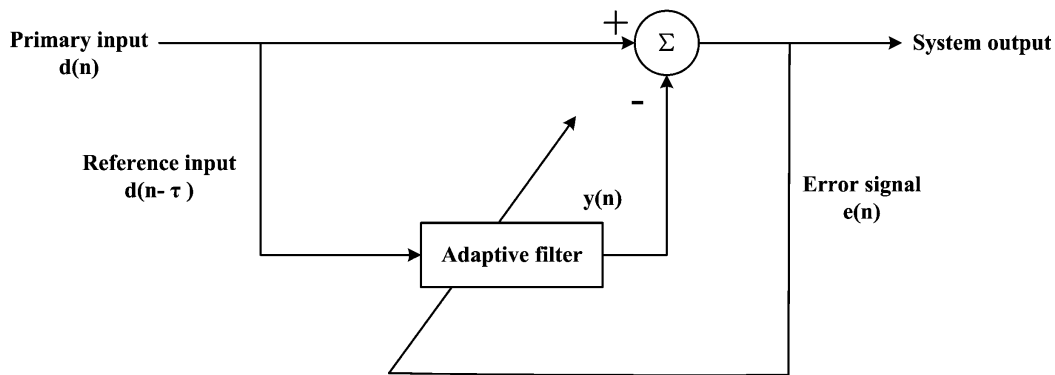


**Figure 10.** Block diagram of the adaptive line enhancer.

The primary input signal is the noise-contaminated signal. The reference signal is a delayed version of the primary input, and  $\tau$  is the delay time, which should be set less than the time correlated radius. For the adaptive filter, the tap weights of the filter are adapted by means of the Least-Mean-Square (LMS) algorithm [21].

Another process that should be done for the adaptive line enhancer process is the time delay estimation because the ALE processing system can cause some phase change on the input signal. With the estimated time delay, the phase can be calibrated, then the correlation coefficient can be carried out on the calibrated signal and the original signal. Calculate the cross coefficient between the output signal and the original signal, and the maximum of the cross-correlation function indicates the number of points in time where the signals are best aligned [22].

The other algorithm is the Ensemble Empirical Mode Decomposition (EEMD), which represents a substantial improvement over the original Empirical Mode Method (EMD). EMD is a time space analysis method. The noise is cancelled out by ‘sifting’ process, and the left part is treated as the true and more physical meaningful answer. To overcome the mode mixing problem, Ensemble Empirical Mode Decomposition (EEMD) is proposed, which defines the true Intrinsic Mode Function (IMF) as the mean of an ensemble of trials [23, 24]. A flowchart of EEMD is shown in Figure 11.

The sifting process is carried out as:

1. Locate all the extrema (both maxima and minima);
2. Interpolate the maxima and minima points by cubic splines to get the upper and lower envelopes;

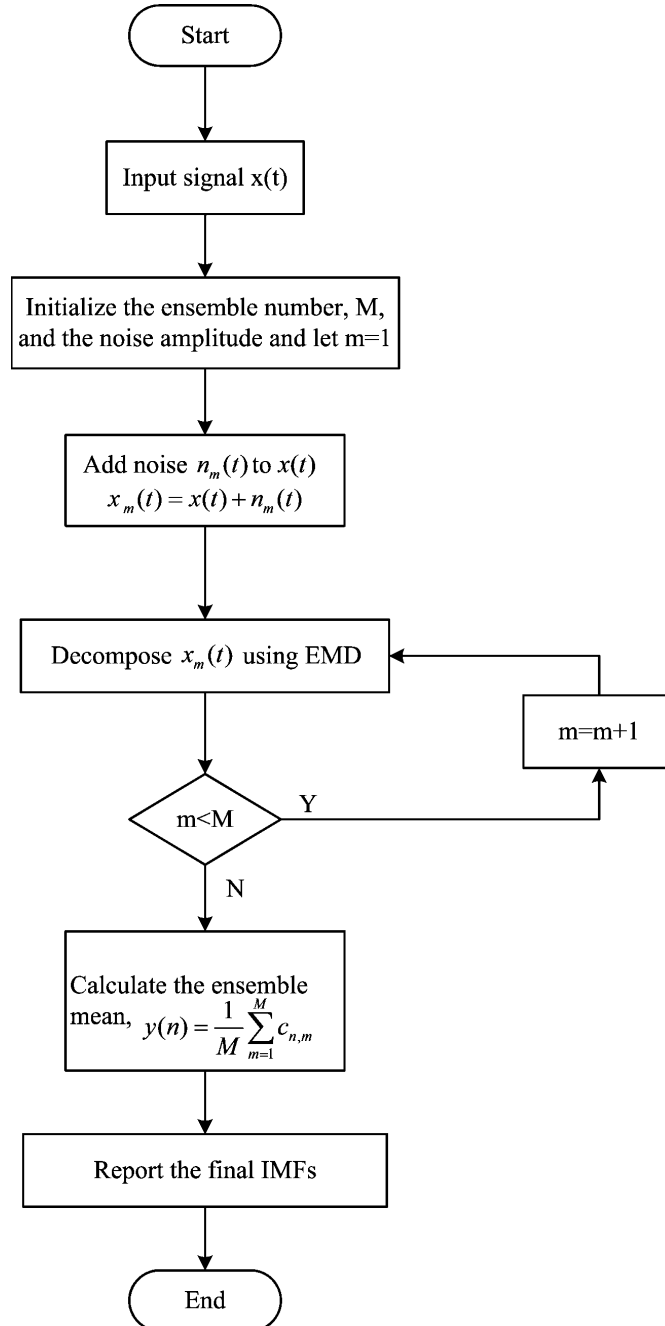


**Figure 11.** Flowchart of ensemble empirical mode decomposition.

3. Subtract the local mean of the upper and lower envelope from the original signal to obtain the first component  $h_1(t)$ ;
4. Test whether  $h_1(t)$  can satisfy the following two IMF conditions. (1). For the whole signal item, the number of extrema is equal to the number of zero crossings, or one difference at the most. (2). At any point, the mean of the maxima envelope and minima envelope should be zero, which means that the signal is symmetric about the time axis.

If  $h_1(t)$  satisfies the two conditions, it will be regarded as the first IMF<sub>1</sub>(t), IMF<sub>1</sub>(t) =  $h_1(t)$ , but if  $h_1(t)$  does not satisfy the conditions,  $h_1(t)$  will be treated as a new signal and repeat steps 1–4 on  $h_1(t)$  for  $k$  times until the two conditions are satisfied, and a new signal  $h_{1k}(t)$  is obtained

$$\text{IMF}_1(t) = h_{1k}(t);$$

5. Subtract  $\text{IMF}_1(t)$  from the original signal and obtain the first order residual signal  $r_2(t)$  and repeat steps (1)–(4) to obtain the  $\text{IMF}_3(t), \dots, \text{IMF}_N(t)$  and the  $r_n(t), r_3(t), \dots, r_N(t)$ . This step

$$\text{can be illustrated as } \begin{cases} r_1(t) - \text{IMF}_1(t) = r_2(t) \\ \vdots \\ r_{N-1} - \text{IMF}_N(t) = r_N(t) \end{cases};$$

6. A complete sifting process stops when the residue,  $r_N(t)$ , becomes a monotonic function from which no more IMF can be extracted.

### 3.2. Result of the Comparison

The result of the comparison is shown in Figure 12. It can be seen that both ALE and EEMD can filter out the noise to an extent (above 0.95). But for each point of standard deviation of  $B$ , the result of EEMD method is better than that of ALE method. The correlation coefficient in the result of ALE is in a decreasing trend along with the increase of the deviation of  $B$ , which can be seen from that the slope of the linear trend of the correlation coefficient is negative, while the result of EEMD is generally in a stable status against the increase of standard deviation of  $B$  as the slope of the linear trend is near 0.

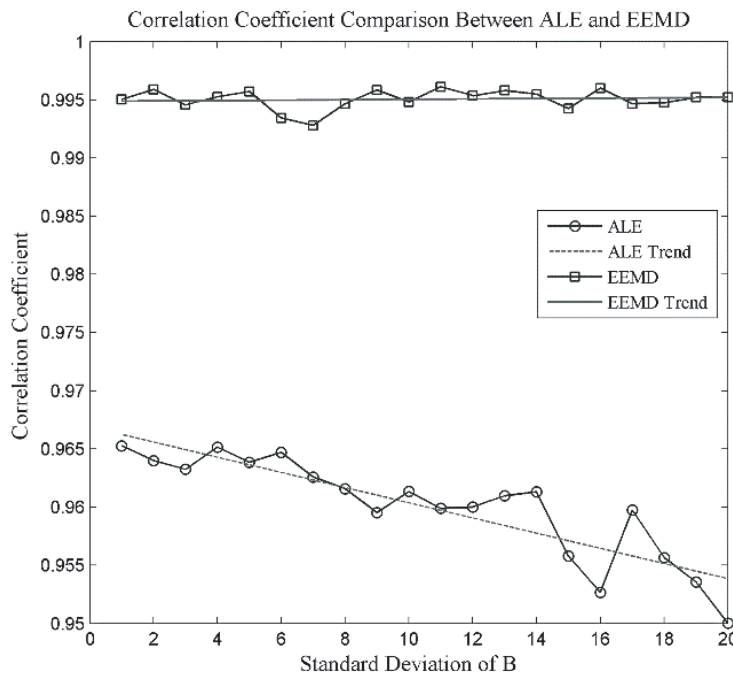


Figure 12. Result of the comparison between the EEMD method and ALE method.

## 4. DISCUSSION

In the model setup process, the morphology model can follow the change of the real respiratory signal by changing the parameters in the structure element, which is verified by that the correlation coefficient can reach 0.98. The change of the morphological shape is achieved by the effect of the structure element with the derivative of the time signal, which can keep the morphological change from the elimination effect of scaling process. In order to simplify the model and lower the number of parameters, an examination is carried out with  $A$  in the structure element being a fixed number and optimizing  $B$  in the structure

element to mimic the real respiratory signal. The correlation coefficient can reach 0.96, better than the result of original PACM model, which is 0.81, worse than the result with both optimized  $A$  and  $B$ . The experiment result proves the efficiency of the proposed model.

An experiment with the simulated respiratory signal is carried out to study the effect of the parameters in the model on the detection algorithms. Two algorithms are used. One is the adaptive line enhancer (ALE), and the other is ensemble empirical mode decomposition (EEMD). The results show that both of the algorithms can achieve the goal of de-noising, with the correlation coefficient above 0.95. However, the EEMD method shows better performance than the ALE method, proved by that the correlation coefficient of the EEMD keeps higher than that of the ALE method. Furthermore, the correlation coefficient in the result of ALE method is in a decreasing trend against the increase of the deviation of  $B$ , while that in the result of EEMD method keeps stable, with a high value (average being 0.995). As the deviation of the parameters in the structure element can be a measure of non-linearity and non-stationarity, the result indicates that the EEMD method has a better performance over the ALE method with the increase of the non-linearity and non-stationarity of the respiratory signal.

## 5. CONCLUSION

This paper presents a morphological method based respiratory signal modeling. It pays attention to the time domain information compared with the previous modeling methods. The experiment shows that it can mimic the real respiratory signal sensed by IR-UWB radar. It is a good method to simulate the respiratory signal, which is promising in the area of simulation and the test of human target detection algorithm. Because the model is a time domain method, the parameters can be treated as a measure of non-linearity and non-stationarity of the sensed respiration. The comparison result shows that the EEMD has better performance than the ALE method, which indicates that the EEMD based human detection algorithm has a good property to resist the non-linearity and non-stationarity.

## ACKNOWLEDGMENT

This research was supported by the National Natural Science Foundation of China (Grant No. 61327805).

**Author Contributions:** Each author contributed extensively to this project. Miao Liu, Huijun Xue and Fulai Liang designed the experiment; Hao Lv and Zhao Li offered help on the realization of detection algorithm; Fugui Qi and Ziqi Zhang helped to carry out the experiment and collect data. Jianqi Wang revised and improved the paper writing.

**Conflicts of Interest:** The authors declare no conflict of interest.

## REFERENCES

1. Lazaro, A., D. Girbau, and R. Villarino, "Analysis of vital signs monitoring using an IR-UWB radar," *Progress In Electromagnetics Research*, Vol. 100, 265–284, 2010.
2. Chang, S., N. Mitsumoto, and J. W. Burdick, "An algorithm for UWB radar-based human detection," *IEEE Radar Conference, 2009*, 1–6, IEEE, Pasadena, CA, USA, May 4–8, 2009.
3. Yarovoy, A. G., L. P. Ligthart, J. Matuzas, and B. Levitas, "UWB radar for human being detection," *IEEE Aerospace and Electronic Systems Magazine*, Vol. 21, 22–26, 2006.
4. Liu, L., Z. Liu, and B. E. Barrowes, "Through-wall bio-radiolocation with UWB impulse radar: Observation, simulation and signal extraction," *IEEE J-STARs*, Vol. 4, 791–798, 2011.
5. Li, Z., W. Li, H. Lv, Y. Zhang, X. Jing, and J. Wang, "A novel method for respiration-like clutter cancellation in life detection by dual-frequency IR-UWB radar," *IEEE Transactions on Microwave Theory and Techniques*, Vol. 61, 2086–2092, 2013.
6. Liu, M., S. Li, H. Lv, Y. Tian, G. Lu, Y. Zhang, Z. Li, W. Li, X. Jing, and J. Wang, *Human Detection Algorithm Based on Bispectrum Analysis for IR-UWB Radar*, 674–681, Springer Berlin Heidelberg, 2013.

7. Li, J., L. Liu, Z. Zeng, and F. Liu, "Advanced signal processing for vital sign extraction with applications in UWB radar detection of trapped victims in complex environments," *IEEE Journal of Selected Topics in Applied Earth Observations and Remote Sensing*, Vol. 7, 783–791, 2014.
8. Mabrouk, M., S. Rajan, M. Bolic, I. Batkin, H. R. Dajani, and V. Z. Groza, "Detection of human targets behind the wall based on singular value decomposition and skewness variations," *IEEE Radar Conference 2014*, 1466–1470, IEEE, Cincinnati, OH, USA, May 19–23, 2014.
9. Sengupta, S. K., *Fundamentals of Statistical Signal Processing: Estimation Theory*, 465–466, PTR Prentice Hall, 1993.
10. Li, X., D. Qiao, and Y. Li, "An analytical model for regular respiratory signal," *Conf. Proc. IEEE Eng. Med. Biol. Soc.*, 102–105, 2014.
11. Serra, J., *Image Analysis and Mathematical Morphology*, 536, Academic Press, 1982.
12. Zhang, F. and Y. Lian, "QRS detection based on multiscale mathematical morphology for wearable ECG devices in body area networks," *IEEE Transactions on Biomedical Circuits and Systems*, Vol. 3, 220, 2009.
13. Xu, G., J. Wang, Q. Zhang, S. Zhang, and J. Zhu, "A spike detection method in EEG based on improved morphological filter," *Computers in Biology and Medicine*, Vol. 37, 1647, 2007.
14. Dogdas, B., D. W. Shattuck, and R. M. Leahy, "Segmentation of skull and scalp in 3-D human MRI using mathematical morphology," *HUM BRAIN MAPP*, Vol. 26, 273–285, 2005.
15. Nezirovic, A., A. G. Yarovoy, and L. P. Ligthart, "Experimental study on human being detection using UWB radar," *IEEE International Radar Symposium 2006, IRS 2006*, 1–4, 2006.
16. Karlen, W., S. Raman, J. M. Ansermino, and G. A. Dumont, "Multiparameter respiratory rate estimation from the photoplethysmogram," *IEEE Trans. Biomed. Eng.*, Vol. 60, 1946–1953, 2013.
17. Chang, C. and G. H. Glover, "Relationship between respiration, end-tidal CO<sub>2</sub>, and BOLD signals in resting-state fMRI," *NEUROIMAGE*, Vol. 47, 1381–1393, 2009.
18. Lv, H., W. Li, Z. Li, Y. Zhang, T. Jiao, H. Xue, M. Liu, X. Jing, and J. Wang, "Characterization and identification of IR-UWB respiratory-motion response of trapped victims," *IEEE Transactions on Geoscience and Remote Sensing*, Vol. 52, 7195–7204, 2014.
19. Lv, H., T. Jiao, Y. Zhang, Q. An, M. Liu, F. Liang, X. Jing, and J. Wang, "An adaptive-MSSA-based algorithm for detection of trapped victims using UWB radar," *IEEE Geoscience and Remote Sensing Letters*, Vol. 12, 1808–1812, 2015.
20. Reddy, V. U. and A. Nehorai, "Response of adaptive line enhancer to a sinusoid in lowpass noise," *IEE Proceedings F — Communications, Radar and Signal Processing*, Vol. 128, 161–166, 1981.
21. Li, W. Z., Z. Li, H. Lv, G. Lu, Y. Zhang, X. Jing, S. Li, and J. Wang, "A new method for non-line-of-sight vital sign monitoring based on developed adaptive line enhancer using low centre frequency UWB radar," *Progress In Electromagnetics Research*, Vol. 133, 535–554, 2013.
22. Benesty, J., J. D. Chen, and Y. T. Huang, "Time-delay estimation via linear interpolation and cross correlation," *IEEE Transactions on Speech and Audio Processing*, Vol. 12, 509–519, 2004.
23. Lei, Y., Z. He, and Y. Zi, "Application of the EEMD method to rotor fault diagnosis of rotating machinery," *Mechanical Systems and Signal Processing*, Vol. 23, 1327–1338, 2009.
24. Wu, Z. and N. E. Huang, "Ensemble empirical mode decomposition: A noise-assisted data analysis method," *Advances in Adaptive Data Analysis*, Vol. 1, 1–41, 2011.